Yttrium-organic framework based on hexagonal prism second building unit for luminescent sensing antibiotics and highly effective CO_2 fixation

Yu Ye, Bangdi Ge, Xianyu Meng, Yuchuan Liu, Shun Wang, Xiaowei Song* and Zhiqiang Liang*

State Key Laboratory of Inorganic Synthesis and Preparative Chemistry, Jilin University, Changchun 130012, P. R. China

*Corresponding Authors.

E-mail addresses: xiaoweisong@jlu.edu.cn (X. W. Song), liangzq@jlu.edu.cn (Z. Q. Liang).

Materials and characterizations

All the chemicals used in the synthesis were purchased and not further purified. 2,3,5,6-tetrakis (4-carboxyphenyl)pyrazine (H_4TCPP) was synthesized by our previous work. Powder X-ray diffraction (PXRD) patterns were collected on a Rigaku D-Max 2550 diffractometer using Cu−Kα radiation (λ = 0.15418 nm) in a 2θ range of 4−40° with a scan speed of 6° min^{-1} at room temperature. The elemental analyses (C, H, and N) were collected on a vario MICRO elemental analyzer. Thermogravimetric analyses (TGA) were achieved on a TGA Q500 thermogravimetric analyser, the measure temperature is from 30-800 °C in air, and the heating rate is 10 °C min^{-1}. The N_2 adsorption measurements were measured on Micromeritics 3-Flex instruments. The CO_2 gas adsorption isotherms were measured on a Micromeritics ASAP 2020. ^{1}H NMR spectra were collected on a Varian 300 MHz NMR spectrometer.

Crystal structure determination

Crystallographic data were harvested using a Bruker D8 VENTURE diffractometer through a graphite monochromated Mo-Kα (λ = 0.71073 Å) radiation at 200 K. Data processing was obtained using the SAINT processing program. The structures were solved through direct method and refined on F^2 by full-matrix least squares with the SHELX-2016 program package. All the non-hydrogen atoms were refined with anisotropic thermal parameters, while hydrogen atoms on the aromatic rings were placed geometrically with isotropic thermal parameters 1.2 times that of the attached carbon atoms. Due to the existence of highly disordered solvent molecules in the cavities, there are some Q peaks with high-electron density for all three compounds in the final structure refinement, which cannot be confirmed accurately. Therefore, the SQUEEZE routine was used for the removal of diffused electron densities. Detailed refinement information could be checked from the CIF file. A summary of the related crystallographic date and structure refinement parameters for **Y-MOF** could be found in Table S1. The asymmetric unit of **Y-MOF** is plotted in Fig. S1.

CCDC 2041740 contains the supplementary crystallographic data for this paper. These data can be obtained free of charge via www.ccdc.cam.ac.uk/data_request/cif, or by emailing data_request@ccdc.cam.ac.uk, or by contacting The Cambridge Crystallographic Data Centre, 12 Union Road, Cambridge CB2 1EZ, UK; fax: +44 1223 336033.

Table S1. Crystal data and structure optimization data for **Y-MOF.**

Name	**Y-MOF**
Formula	$C_{96}H_{48}N_6O_{50}Y_9$
Formula weight	2885.59
Temperature	200(2) K
Wavelength	0.71073 Å
Crystal system	Hexagonal
Space group	*P6₃/mmc*
Unit cell dimensions	a = 21.6964(4) Å α= 90°. b = 21.6964(4) Å β= 90°. c = 24.8326(12) Å γ = 120°.
Volume	10123.4(6) Å^3
Z	2
Density (calculated)	0.947 g/cm^3
Absorption coefficient	2.599 mm^{-1}
F(000)	2834
Crystal size	0.1 × 0.1 × 0.1 mm
Theta range for data collection	2.318 to 25.031°
Reflections collected/ unique	67677 / 3315
R_{int}	0.0262
Completeness to theta= 25.242°	99.4 %
Refinement method	Full-matrix least-squares on F^2
Data / restraints / parameters	3315 / 90 / 136
Goodness-of-fit on F^2	1.158
[a]R_1, wR_2 [I >2σ (I)]	R_1 = 0.0725, wR_2 = 0.3091
R_1, wR_2 (all data)	R_1 = 0.0742, wR_2 = 0.3308
Extinction coefficient	n/a
Largest diff. peak and hole	3.878 and -1.630 e.·Å^{-3}

Table S2. Selected bond lengths [Å] and angles [°] for **Y-MOF.**.

O(1)-Y(1)	2.26427(3)	O(2)-Y(1)-O(1)	84.2
O(2)-Y(1)	2.17949(10)	O(4)#3-Y(1)-O(1)	79.008(1)
O(3)-Y(1)#3	2.26607(4)	O(4)-Y(1)-O(1)	150.6
O(3)-Y(1)#4	2.266069(11)	O(2)-Y(1)-O(1)#1	84.200(1)
O(3)-Y(1)	2.26609(4)	O(4)#3-Y(1)-O(1)#1	150.6
O(4)-Y(1)	2.25939(6)	O(4)-Y(1)-O(1)#1	79
O(4)-Y(1)#4	2.259386(15)	O(1)-Y(1)-O(1)#1	73.492(1)
O(4)-Y(2)	2.55789(7)	O(2)-Y(1)-O(3)	94.067(1)
O(5)-Y(2)	2.22184(5)	O(4)#3-Y(1)-O(3)	64.279(1)
O(5)-Y(1)	2.27906(8)	O(4)-Y(1)-O(3)	64.277(1)
O(5)-Y(1)#5	2.27906(10)	O(1)-Y(1)-O(3)	143.1
O(6)-Y(1)#5	2.58370(10)	O(1)#1-Y(1)-O(3)	143.1
O(7)-Y(2)	2.24564(7)	O(2)-Y(1)-O(5)#1	148.040(1)
O(8)-Y(2)	2.41075(5)	O(4)#3-Y(1)-O(5)#1	67.354(1)
C(1)-O(1)-Y(1)	134.8	O(4)-Y(1)-O(5)#1	123.399(1)
Y(1)#3-O(3)-Y(1)#4	113.997(1)	O(1)-Y(1)-O(5)#1	79.033(2)
Y(1)#3-O(3)-Y(1)	114	O(1)#1-Y(1)-O(5)#1	116.1
Y(1)#4-O(3)-Y(1)	113.998(1)	O(3)-Y(1)-O(5)#1	83.714(1)
Y(1)-O(4)-Y(1)#4	114.522(1)	O(2)-Y(1)-O(5)	148.039(1)
Y(1)-O(4)-Y(2)	107.4	O(4)#3-Y(1)-O(5)	123.402(1)
Y(1)#4-O(4)-Y(2)	107.417(2)	O(4)-Y(1)-O(5)	67.353(1)
Y(2)-O(5)-Y(1)	119.433(1)	O(1)-Y(1)-O(5)	116.1
Y(2)-O(5)-Y(1)#5	119.432(2)	O(1)#1-Y(1)-O(5)	79.031(2)
Y(1)-O(5)-Y(1)#5	115.010(3)	O(3)-Y(1)-O(5)	83.715(2)
C(1)#1-O(7)-Y(2)	141.529(1)	O(5)#1-Y(1)-O(5)	63.609(2)
O(2)-Y(1)-O(4)#3	82.9	O(5)-Y(2)-O(5)#7	85.3
O(2)-Y(1)-O(4)	82.9	O(5)-Y(2)-O(7)#8	136.184(2)
O(4)#3-Y(1)-O(4)	125.1	O(5)#7-Y(2)-O(7)#8	79.376(1)

O(5)#7-Y(2)-O(7)#5	136.184(1)	O(5)#7-Y(2)-O(4)	63.081(1)
O(7)#8-Y(2)-O(7)#5	83.903(3)	O(7)#8-Y(2)-O(4)	137.339(2)
O(5)-Y(2)-O(7)#7	136.184(1)	O(7)#5-Y(2)-O(4)	137.339(1)
O(5)#7-Y(2)-O(7)#7	79.376(1)	O(7)#7-Y(2)-O(4)	73.397(2)
O(7)#8-Y(2)-O(7)#7	80.761(3)	O(7)-Y(2)-O(4)	73.397(3)
O(7)#5-Y(2)-O(7)#7	137.158(1)	O(8)-Y(2)-O(4)	127.995(1)
O(5)-Y(2)-O(7)	79.4	O(5)-Y(2)-O(4)#5	63.081(1)
O(5)#7-Y(2)-O(7)	136.183(2)	O(5)#7-Y(2)-O(4)#5	63.083(1)
O(7)#8-Y(2)-O(7)	137.158(1)	O(7)#8-Y(2)-O(4)#5	73.398(2)
O(7)#5-Y(2)-O(7)	80.761(3)	O(7)#5-Y(2)-O(4)#5	73.395(3)
O(7)#7-Y(2)-O(7)	83.903(3)	O(7)#7-Y(2)-O(4)#5	137.341(1)
O(5)-Y(2)-O(8)	137.343(1)	O(7)-Y(2)-O(4)#5	137.338(2)
O(5)#7-Y(2)-O(8)	137.3	O(8)-Y(2)-O(4)#5	127.994(1)
O(7)#8-Y(2)-O(8)	68.579(1)	O(4)-Y(2)-O(4)#5	104.012(2)
O(7)#5-Y(2)-O(8)	68.579(1)		
O(7)#7-Y(2)-O(8)	68.579(1)		
O(7)-Y(2)-O(8)	68.580(1)		
O(5)-Y(2)-O(4)	63.081(1)		

Symmetry transformations used to generate equivalent atoms:

#1 -y+1,-x+1,z #2 x-y,-y,-z+1 #3 -y+1,x-y-1,z

#4 -x+y+2,-x+1,z #5 x,y,-z+3/2 #6 -x+y+1,y,z

#7 -x+y+2,y,z #8 -x+y+2,y,-z+3/2

#9 -x+y+2,-x+1,-z+3/2

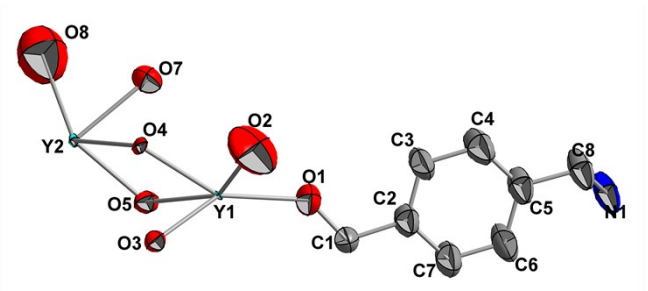

Fig. S1 Representation of the asymmetric unit of **Y-YCPP** showing ellipsoid at the 50% probability level.

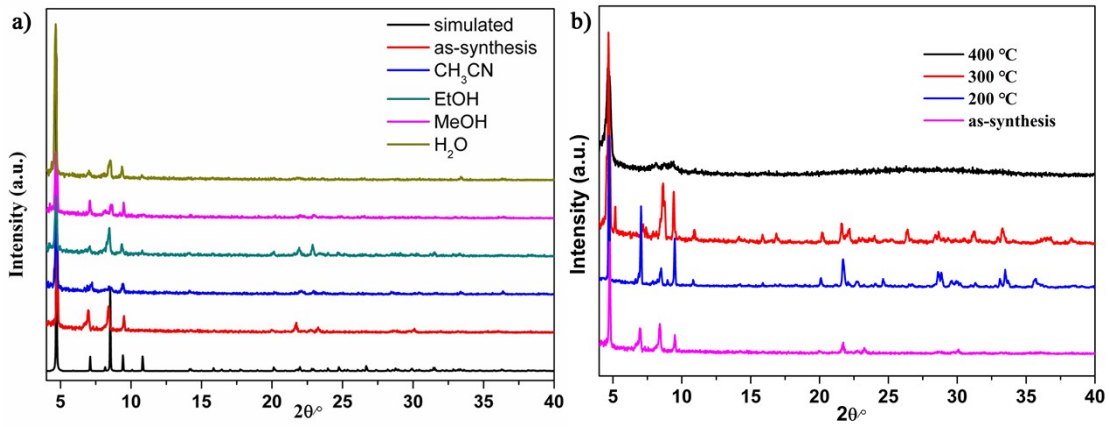

Fig. S2 Powder X-ray diffraction patterns of as-synthesized **Y-YCPP** and (a)soaked in different organic solvent. (b) calcined at different temperatures.

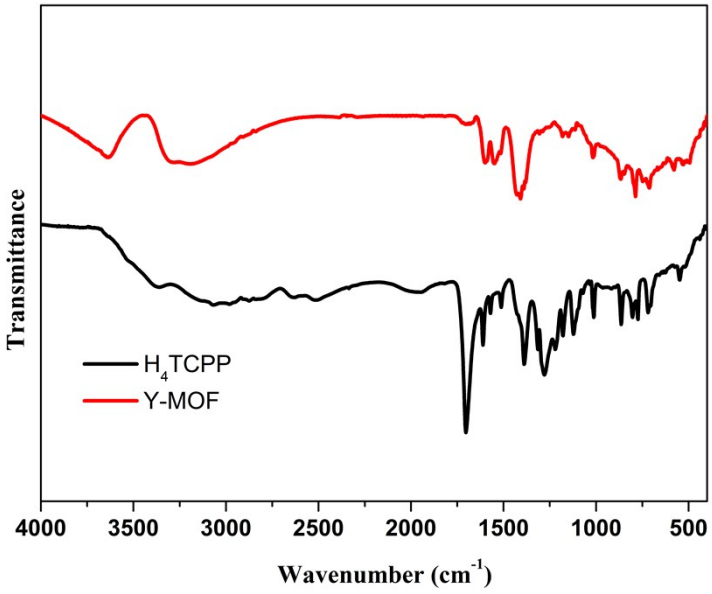

Fig. S3 IR spectra of H_4TCPP and **Y-YCPP.**

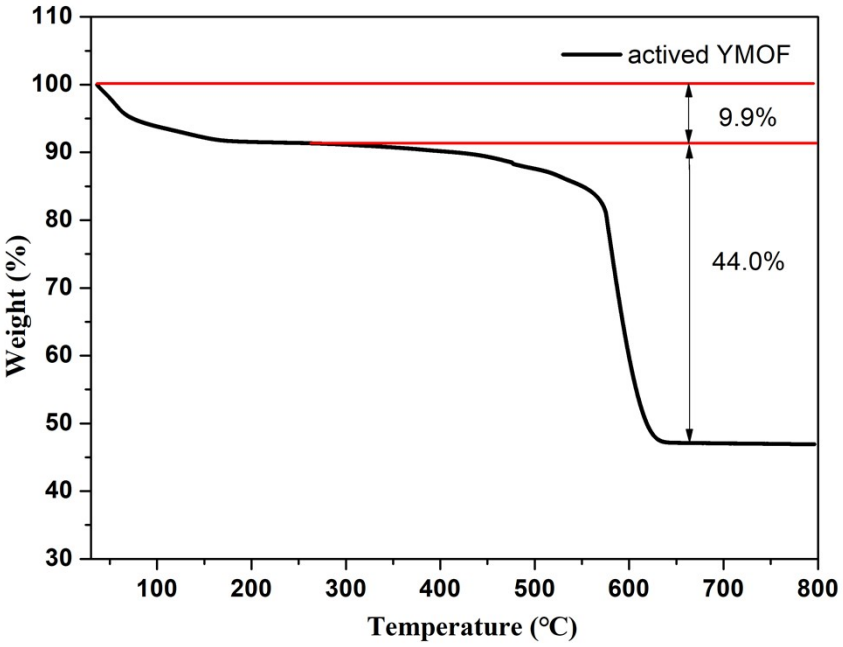

Fig. S4 TGA curves for the activated **Y-YCPP.**

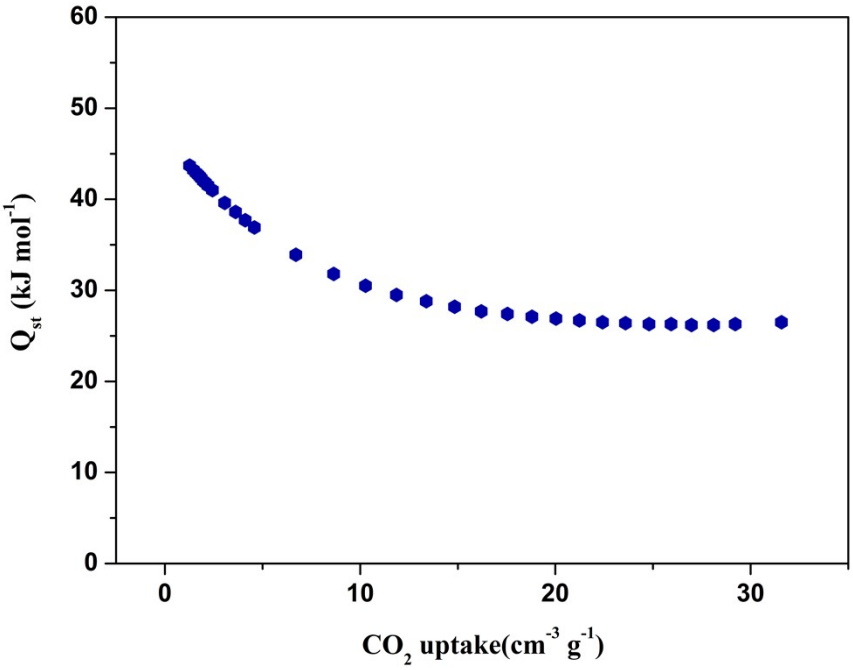

Fig. S5 Isosteric heats of CO_2 adsorption for **Y-TCPP**.

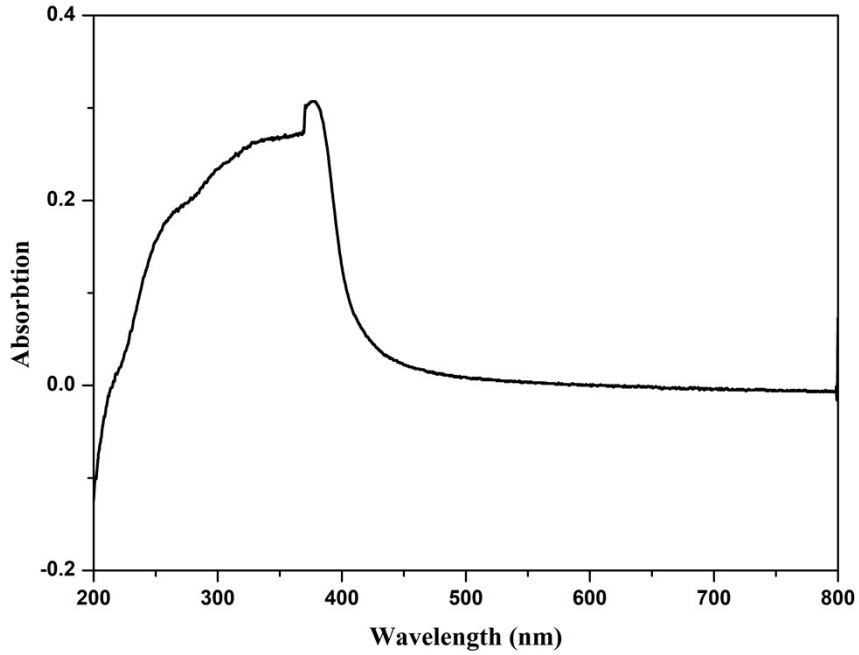

Fig. S6 UV-visible absorption spectrum of solid **Y-TCPP**.

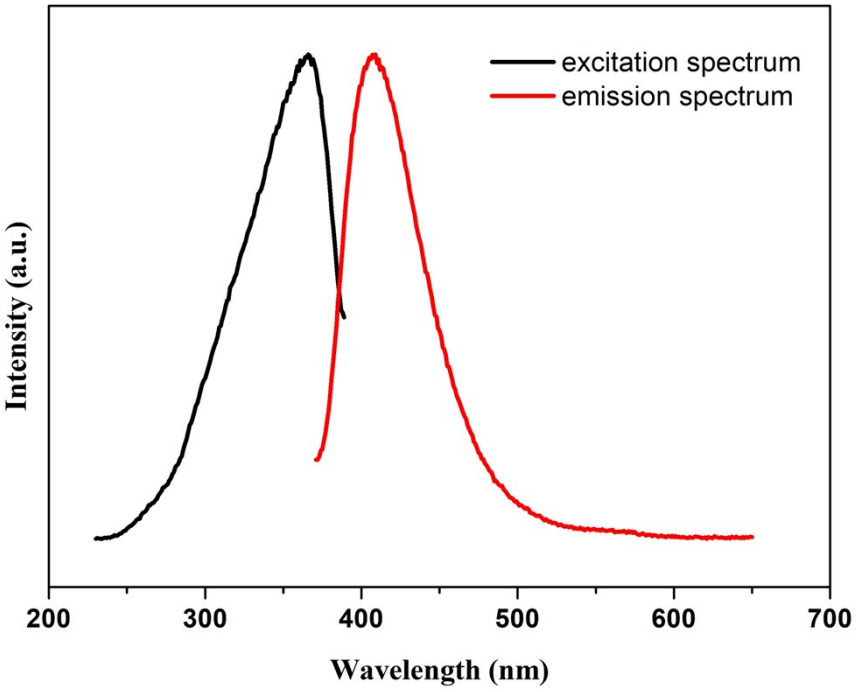

Fig. S7 Luminescent properties of solid **Y-TCPP**.

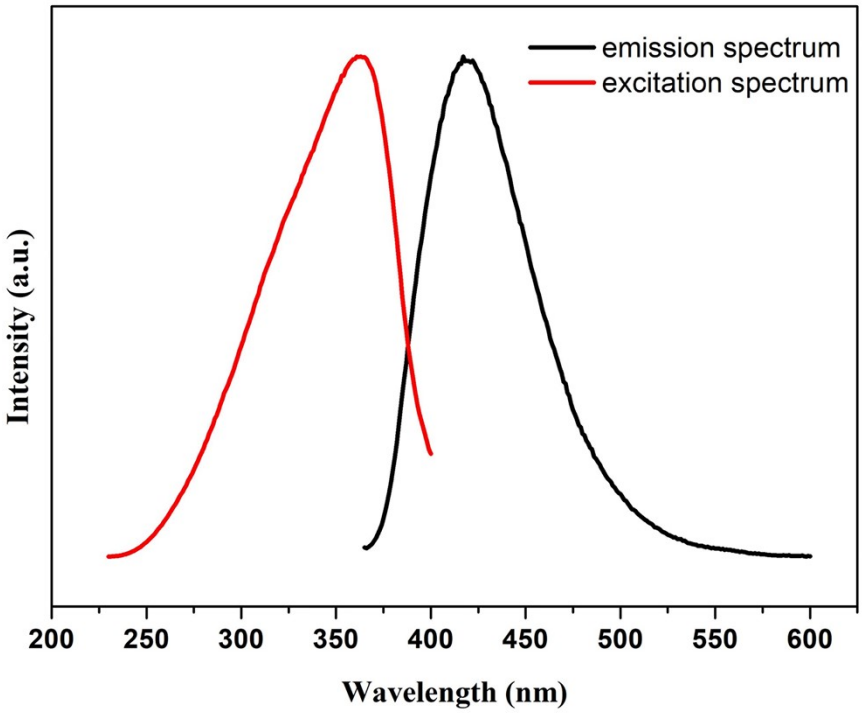

Fig. S8 Luminescent properties of **Y-TCPP** dispersed in water.

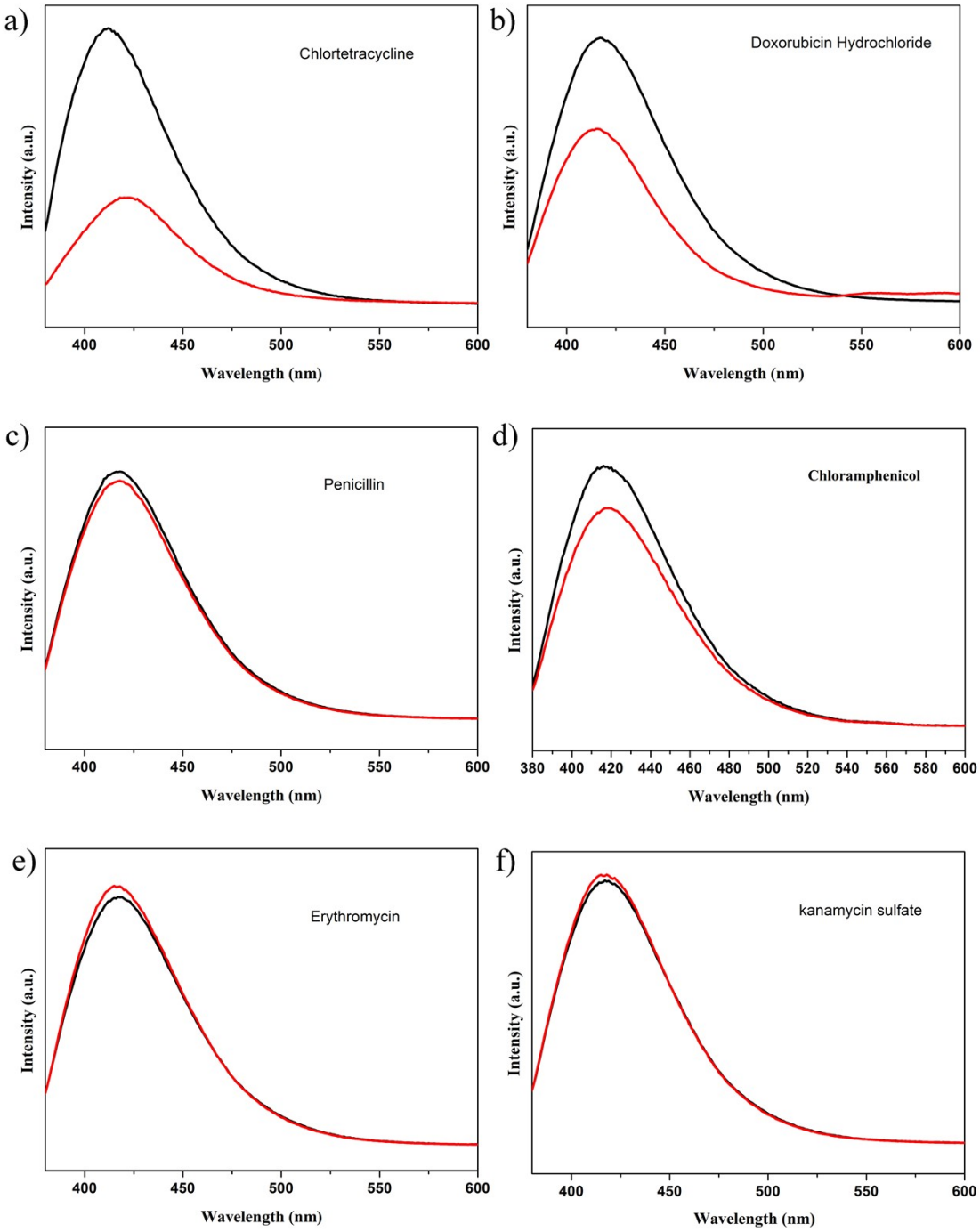

Fig. S9 The fluorescence spectrum of **Y-TCPP** after adding different antibiotics to the **Y-TCPP** suspension.

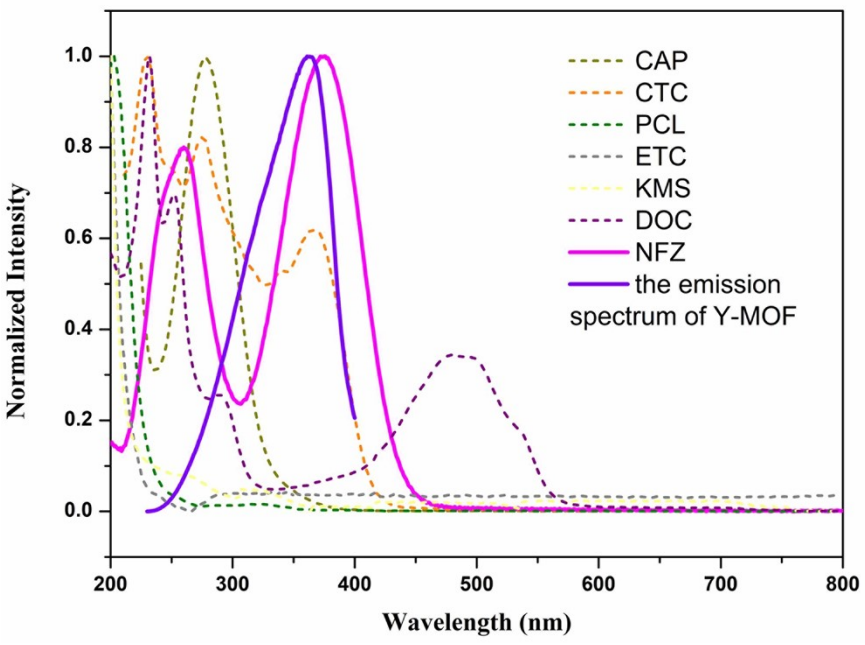

Fig. S10 The emission spectrum of MOF and the UV-visible absorption spectrum of different analytes.

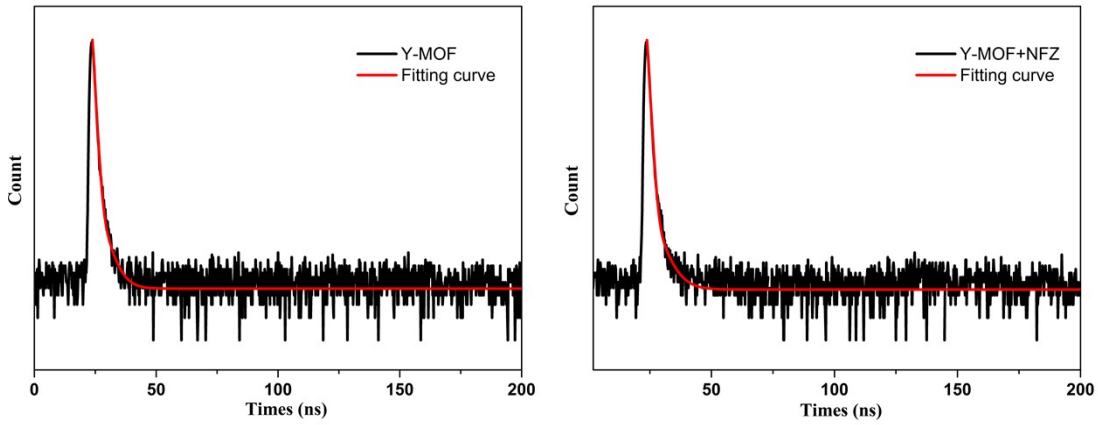

Fig. S11 Time-resolved fluorescence decay spectra of **Y-TCPP** before and after adding NFZ.

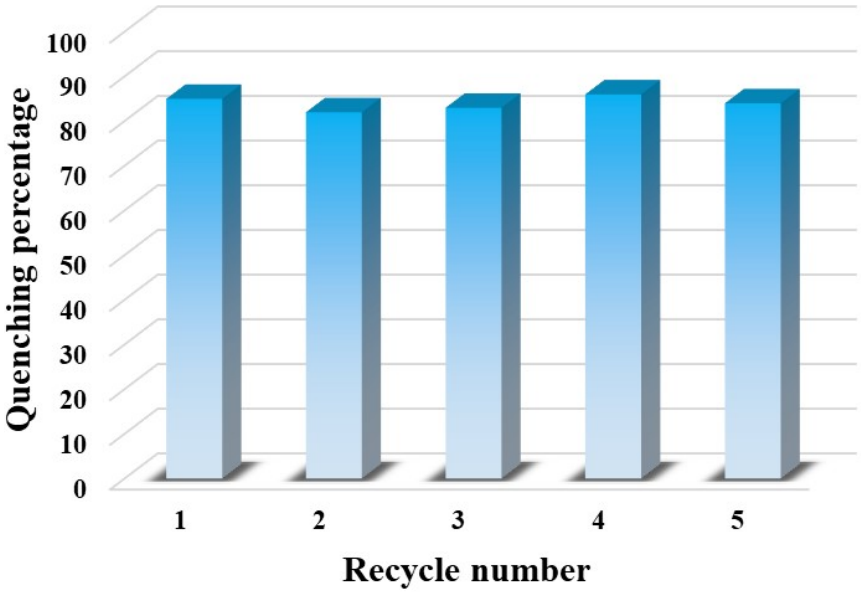

Fig. S12 Reproducibility of the detection effect of **Y-TCPP** after five cycles.

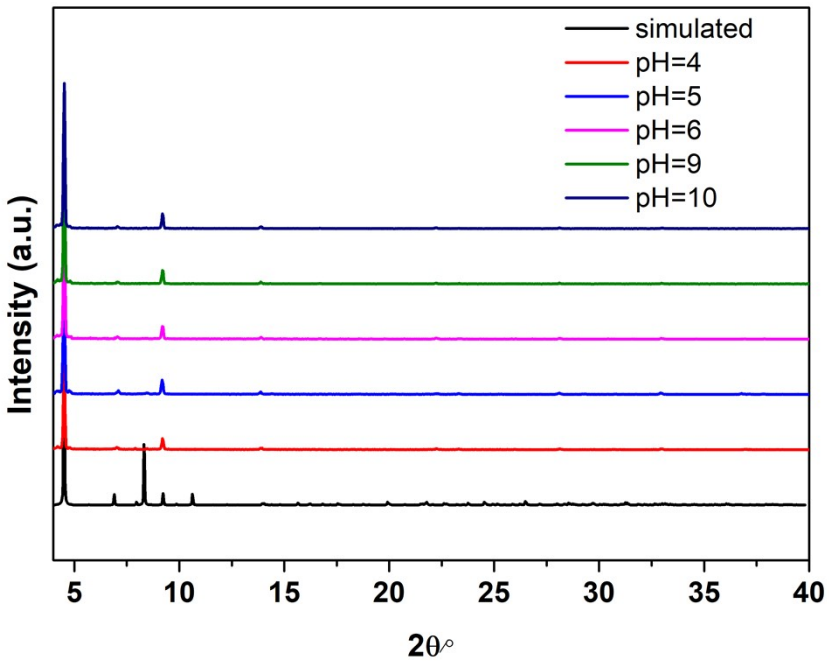

Fig. S13 The PXRD pattern and fluorescence pattern of **Y-TCPP** after being immersed in different pH aqueous solutions for 24 hours

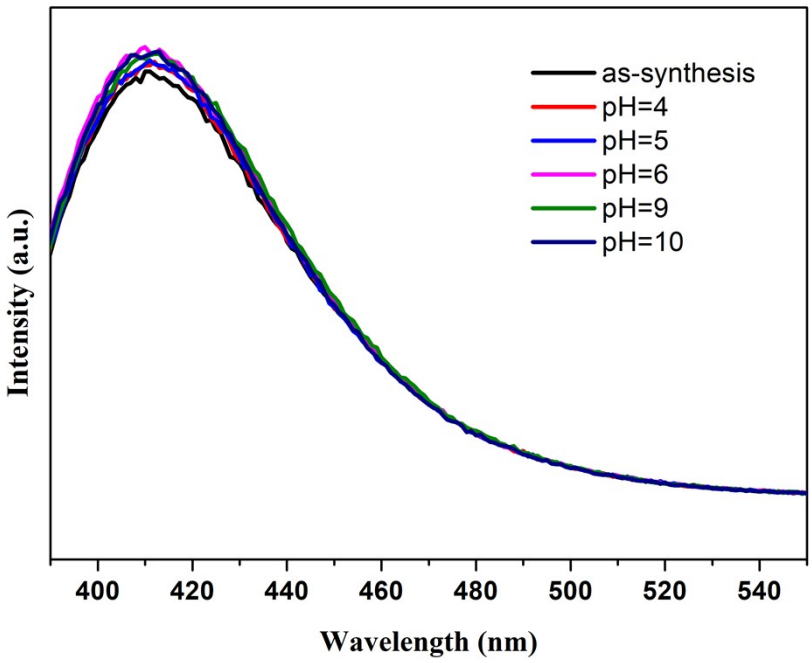

Fig. S14 The fluorescence spectrum of **Y-TCPP** after being immersed in different pH aqueous solutions for 24 hours

With styrene epoxide as a model reactant, the yield was determined by calculation of the ^{1}H NMR integrals of the corresponding highlighted protons in styrene epoxide (H_a), styrene carbonate ($H_{a'}$) and the phenyl group ($H_{b\text{-}f}$) (Fig. S10, as styrene epoxide and styrene carbonate are known compounds, the characteristic peaks were pointed out according to references).[1-3]

$$Yield\ (\%) = \left(\frac{5I_{H_{a'}}}{I_{H_{b-f}}} \right) \times 100\%$$

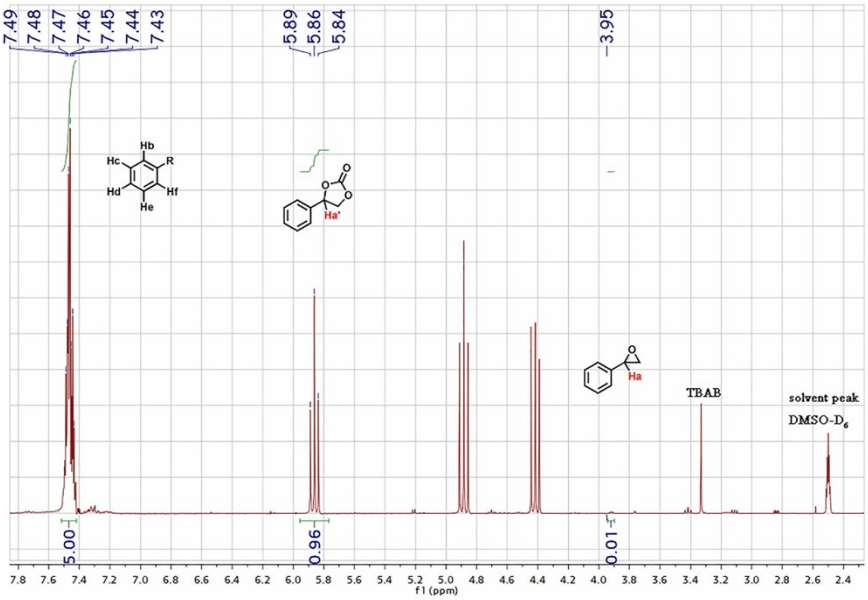

Fig. S15 ^{1}H NMR spectrum of the mixture products by cycloaddition reaction of styrene epoxide to styrene carbonate catalyzed by **Y-TCPP** in DMSO-d_6.

The yields of propylene oxide, epichlorohydrin, allyl glycidyl ether, phenyl glycidyl ether and cresyl glycidyl ether to corresponding cyclic carbonates catalyzing by Y-MOF were calculated with the reported method according to the following equation. (Fig. S12-16, as all of the epoxides and cyclic carbonates are known compounds, the characteristic peaks were pointed out according to references). [1-3]

$$Yield(\%) = \frac{I_{H_{a'}}}{I_{H_a} + I_{H_{a'}}} \times 100\%$$

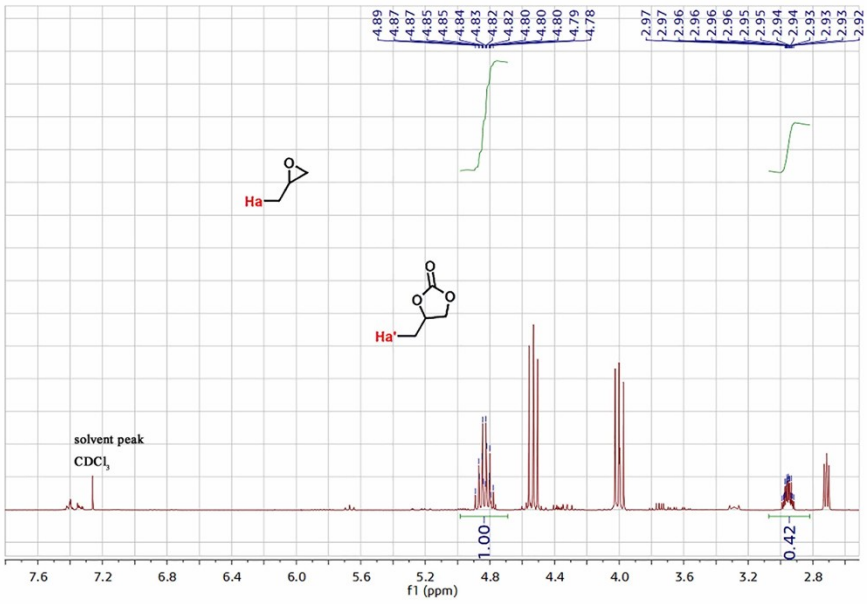

Fig. S16 ^{1}H NMR spectrum of the mixture products by cycloaddition reaction of propylene oxide to propylene carbonate catalyzed by **Y-TCPP** in $CDCl_3$.

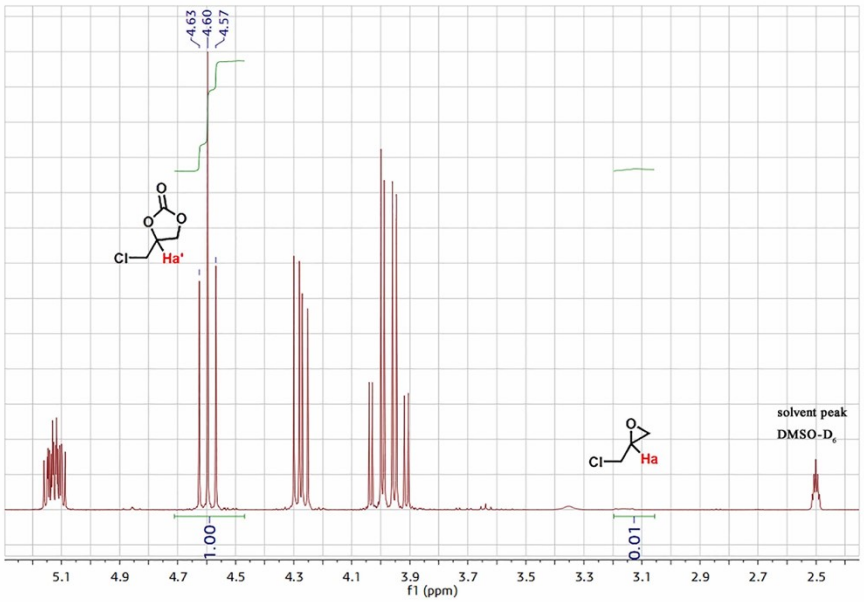

Fig. S17 ^{1}H NMR spectrum of the mixture products by cycloaddition reaction of epichlorohydrin to cycloallyl carbonate catalyzed by **Y-TCPP** in DMSO-d_6.

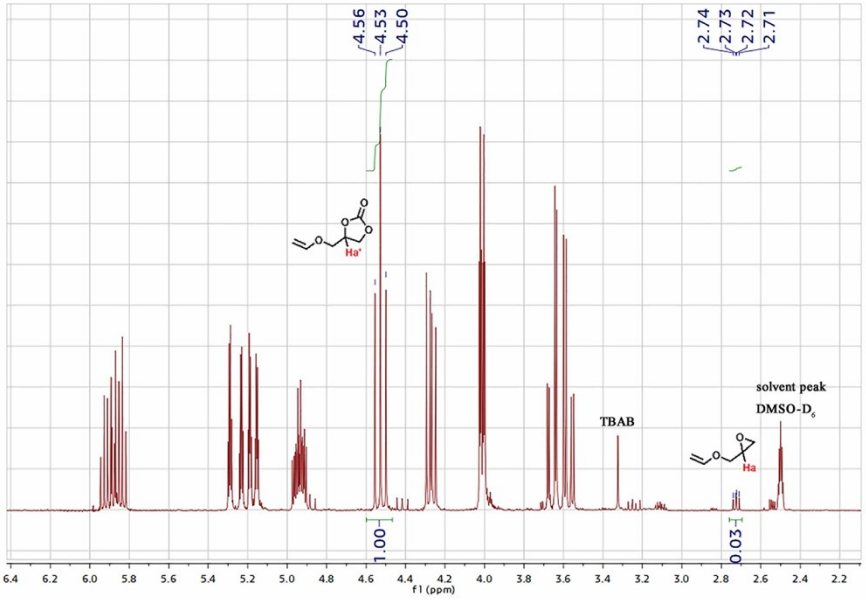

Fig. S18 ^{1}H NMR spectrum of the mixture products by cycloaddition reaction of allyl glycidyl ether catalyzed by **Y-TCPP** in DMSO-d_6.

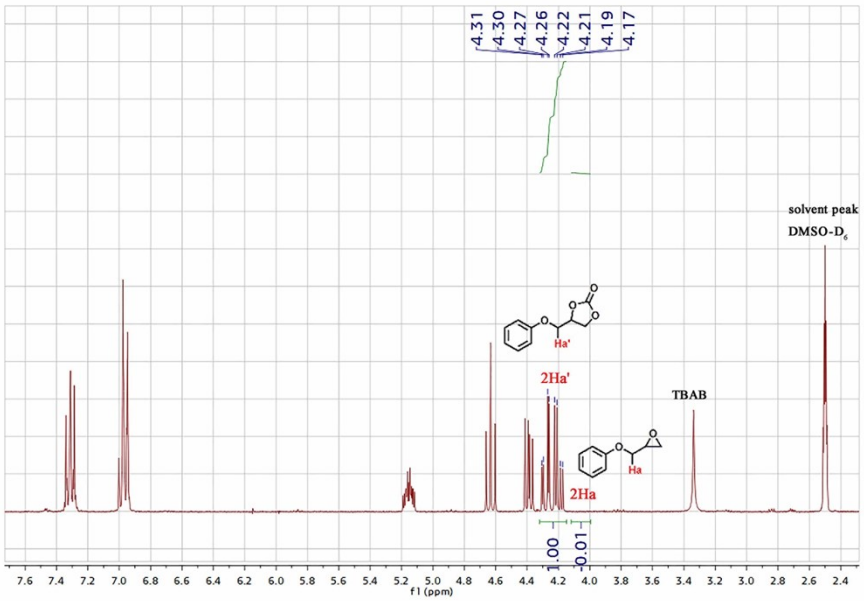

Fig. S19 ^{1}H NMR spectrum of the mixture products by cycloaddition reaction of phenyl glycidyl ether catalyzed by **Y-TCPP** in DMSO-d_6.

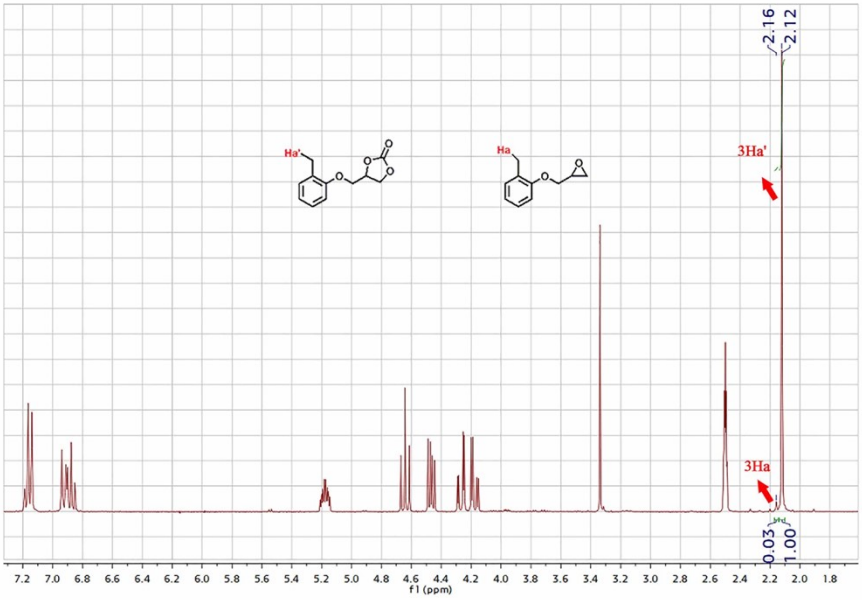

Fig. S20 ^{1}H NMR spectrum of the mixture products by cycloaddition reaction of cresyl glycidyl ether catalyzed by **Y-TCPP** in DMSO-d_6.

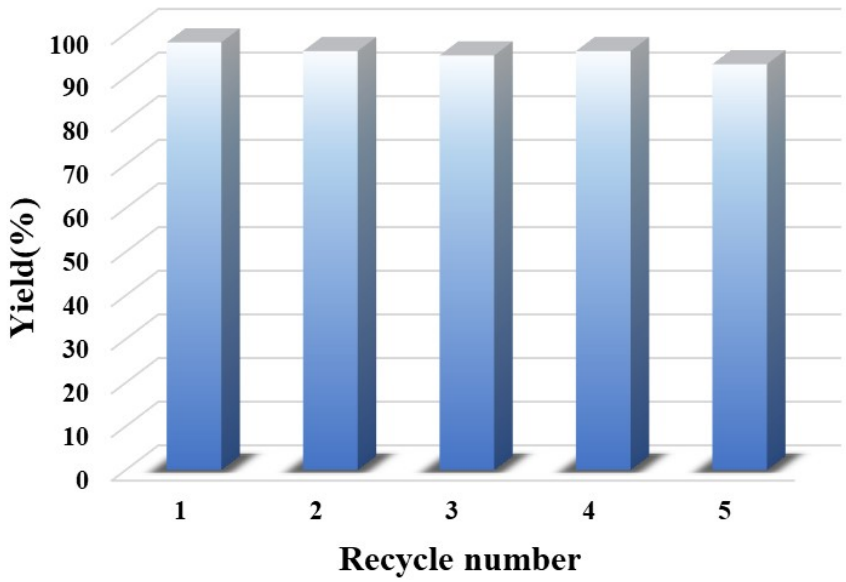

Fig. S21 Recycling of **Y-TCPP** for CO_2 conversion. Conditions: epichlorohydrin (40 mmol), Cat. (10 mg), TBAB (0.37% mmol), CO_2 1 MPa, 100 °C and 4 h.

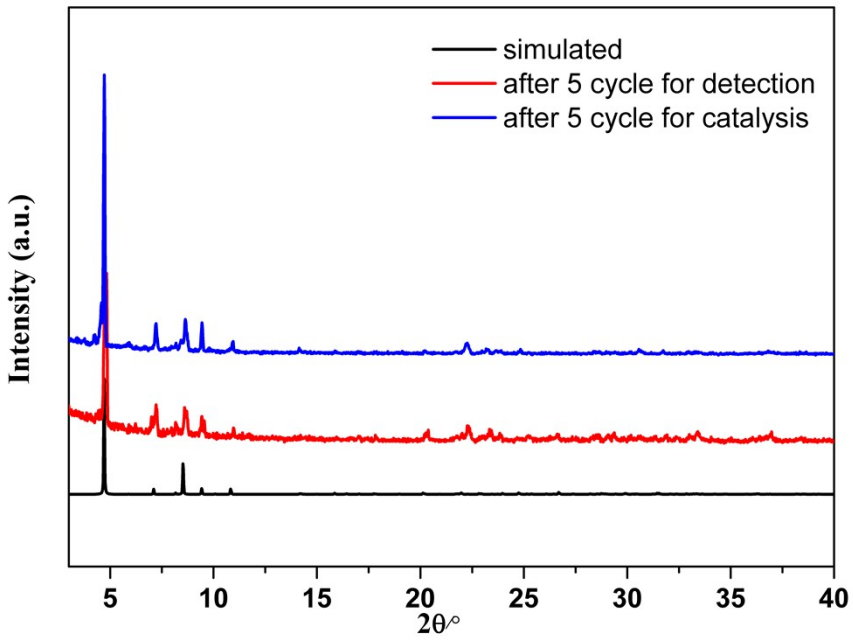

Fig. S22 PXRD patterns of **Y-TCPP** after five rounds of detection and catalysis.

Table S3. Comparisons about fluorescence detection of NFZ with other MOFs.

name	Solvent	LOD	Ksv	Ref.
RhB@Zn-1	EtOH	0.86 μM	4.7×10^4 M^{-1}	4
MOF-76($Eu_{0.04}Tb_{0.96}$)	water	23.0 ppb	2.3×10^4 M^{-1}	5
9A/Cu-atda@Eu^{3+}/SA	water	0.17 μM	3.5×10^4 M^{-1}	6
(TMPyPE@bio-MOF-1	water	0.110ppm	4.5×10^4 M^{-1}	7
Al-MOF	water	0.838μM	1.6×10^4 M^{-1}	8
FCS-5	water	0.22 ppm	3.7×10^4 M^{-1}	9
Eu-MOF 1	water	$1.58*10^{-6}$	2.6×10^4 M^{-1}	10
Zn-MOF	water	4.0x107 mol/L	1.0×10^4 M^{-1}	11
Y-TCPP	water	7.8×10^{-7} M	6.9×10^4 M^{-1}	**This work**

Table S4. Comparisons about CO_2 uptakes under 1 atm at 273 and 298 K of some selected MOFs.

Entry	Cat.	t/h	P/MPa	T/°C	Yield (%)	Ref.
1	DUT-52(Zr)	6	1.2	80	48	12
2	MIL-101-tzmOH-Br	10	1	80	57	13
3	rho-ZMOF	3	1	40	85	14
5	Zn(Bmic)(AT)	6	0.5	80	76	15
7	CSMCRI-13	6	0.8	70	94.5	16
8	$[Cu_2(CPTPTA)(H_2O)]\cdot CH_3NH_3^+\cdot 4H_2O\cdot 7NMF$	6	2	60	65	17
9	F-Mn-MOF-74	6	1	100	99	18
10	Zn(Py)(Atz)	5	1.5	60	66	19
11	Cr-MIL-101	2	2	120	68.5	20
12	JLU-Liu46	6	2	60	96	21
13	UiO-66-BAT	6	0.5	50	82	22
14	Hie-Zn-MOF-TEA(4.0)	3	1	80	41	23
15	**Y-TCPP**	4	1	100	96	**This work**

References

1. S. Yuan, L. F. Zou, H. X. Li, Y.-P. Chen, J. S. Qin, Q. Zhang, W. G. Lu, Michael B. Hall, H.-C. Zhou, Flexible zirconium metal-organic frameworks as bioinspired switchable catalysts, *Angew. Chem. Int. Ed.,* 2016, **55**, 10776–10780.
2. X. D. Sun, J. M. Gu, Y. Yuan, C. Y. Yu, J. T. Li, H. Y. Shan, G. H. Li, Y. L. Liu, A stable mesoporous Zr-based metal organic framework for highly efficient CO_2 conversion, *Inorg. Chem.,* 2019, **58**, 7480–7487.
3. Y. Yuan, J. T. Li, X. D. Sun, G. H. Li, Y. L. Liu, G. Verma, S. Q. Ma, Indium-organic frameworks based on dual secondary building units featuring halogen-decorated channels for highly effective CO_2 fixation, *Chem. Mater.,* 2019, **31**, 1084–1091.
4. Q.-Q. Tu, L.-L. Ren, A.-L. Cheng and E.-Q. Gao, Fabrication of a dual-emitting RhB@Zn-1 composite as a recyclable luminescent sensor for sensitive detection of nitrofuran antibiotics, *CrystEngComm*, 2021, **23**, 629-637.
5. Y. Yang, L. N. Zhao, M. G. Sun, P. P. Wei, G. M. Li and Y. X. Li, Highly sensitive

luminescent detection toward polytypic antibiotics by a water-stable and white-light-emitting MOF-76 derivative, *Dyes Pigm.*, 2020, 108444.

6. K. Zhu, R. Q. Fan, J. Zhang, X. Jiang, W. W. Jia, B. W. Wang, H. Y. Lu, J. K. Wu, P. Wang and Y. L. Yang, Dual-emission 3D supramolecular framework hydrogel beads: highly selective detection of antibiotics and mechanism research, *Dalton Trans.*, 2021, **50**, 15679 –15687.
7. Y.-M. Ying, C.-L. Tao, M. X. Yu, Y. Xiong, C.-R. Guo, X.-G. Liu and Z. J. Zhao, In situ encapsulation of pyridine-substituted tetraphenylethene cations in metal–organic framework for the detection of antibiotics in aqueous medium, *J. Mater. Chem. C*, 2019, **7**, 8383—8388.
8. X. Y. Yue, Z. J. Zhou, M. Li, M. S. Jie, B. C. Xu and Y. H. Bai, Inner-filter effect induced fluorescent sensor based on fusiform Al-MOF nanosheets for sensitive and visual detection of nitrofuran in milk, *Food Chem.*, 2022, **367**, 130763.
9. Z. Lei, L. Hu, Z.-H. Yu, Q.-Y. Yao, X. Chen, H. Li, R.-M. Liu, C.-P. Li and X.-D. Zhu, Ancillary ligand enabled structural and fluorescence diversity in metal–organic frameworks: application for the ultra-sensitive detection of nitrofuran antibiotics, *Inorg. Chem. Front.*, 2021, **8**, 1290 –1296.
10. S.-L. Sun, X. Y. Sun, Q. Sun, E.-Q. Gao, J.-L. Zhang and W.-J. Li, Europium metal-organic framework containing helical metal-carboxylate chains for fluorescence sensing of nitrobenzene and nitrofunans antibiotics, *J. Solid State Chem.*, 2020, **292** 121701.
11. Z. Z. Cong, Z. F. Song, Y. X. Ma, M. C. Zhu, Y. Zhang, S. Y. Wu and E. J. Gao, Highly Emissive Metal-Organic Frameworks for Sensitive and Selective Detection of Nitrofuran and Quinolone Antibiotics, *Chem Asian J.*, 2021, **16**, 1773–1779.
12. J. F. Kurisingal, Y. Rachuri, A. S. Palakkal, R. S. Pillai, Y. Gu, Y. Choe and D.-W. Park, Water-tolerant DUT-series metal−organic frameworks: a theoretical-experimental study for the chemical fixation of CO_2 and catalytic transfer hydrogenation of ethyl levulinate to γ-valerolactone, *ACS Appl. Mater. Interfaces*, 2019, **11**, 41458–41471.
13. L. J. Zhou, W. Sun, N. N. Yang, P. Li, T. Gong, W. J. Sun, Q. Sui and E. Q. Gao, A facile and versatile “click” approach toward multifunctional ionic metal-organic frameworks for efficient conversion of CO_2, *ChemSusChem*, 2019, **12**, 2202–2210.

14. S. Q. Zhang, M. S. Jang, J. Lee, P. Puthiaraj, W. S. Ahn, Zeolite-Like Metal Organic Framework (ZMOF) with a rho Topology for a CO2 Cycloaddition to Epoxides, *ACS Sustainable Chem. Eng.*, 2020, **8**, 7078–7086.
15. Y. Li, X. Zhang, J. Lan, P. Xu and J. Sun, Porous Zn(Bmic)(AT) MOF with abundant amino groups and open metal sites for efficient capture and transformation of CO2, *Inorg. Chem.*, 2019, **58,** 13917–13926.
16. N. Seal and S. Neogi, Intrinsic-unsaturation-enriched biporous and chemorobust Cu(II) framework for efficient catalytic CO_2 fixation and pore-fitting actuated size-exclusive hantzsch condensation with mechanistic validation, *ACS Appl. Mater. Interfaces*, 2021, 10.1021/acsami.1c16984.
17. Y. Y. Zhu, J. M. Gu, X. Y. Yu, B. R. Zhang, G. H. Li, J. T. Li and Y. L. Liu, The multifunctional design of metal–organic framework by applying linker desymmetrization strategy: synergistic catalysis for high CO_2-epoxide conversion, *Inorg. Chem. Front.*, 2021, 10.1039/d1qi00960e.
18. C. Feng, S. S. Qiao, Y. Guo, Y. H. Xie, L. Zhang, N. Akram, S. Li and J. D. Wang, Adenine-assisted synthesis of functionalized F-Mn-MOF-74 as an efficient catalyst with enhanced catalytic activity for the cycloaddition of carbon dioxide, *Colloids Surf. A*, 2020, **597**, 124781.
19. J. W. Lan, Y. Qu, X. Zhang, H. R. Ma, P. Xu and J. M. Sun, A novel water-stable MOF Zn(Py)(Atz) as heterogeneous catalyst for chemical conversion of CO_2 with various epoxides under mild conditions, *J. CO_2 Util.*, 2020, **35**, 216–224.
20. W. L. Dai, P. Mao, Y. Liu, S. Q. Zhang, B. Li, L. X. Yang, X. B. Luo and J. P. Zou, Quaternary phosphonium salt-functionalized Cr-MIL-101: A bifunctional and efficient catalyst for CO_2 cycloaddition with epoxides, *J. CO_2 Util.*, 2020, **36**, 295–305.
21. J. M. Gu, X. D. Sun, X. Y. Liu, Y. Yuan, H. Y. Shan and Y. L. Liu, Highly efficient synergistic CO_2 conversion with epoxide using copper polyhedron-based MOFs with Lewis acid and base sites, *Inorg. Chem. Front.*, 2020, **7**, 4517–4526.
22. A. Helal, M. Usman, M. E. Arafat and M. M. Abdelnaby, Allyl functionalized UiO-66 metal-organic framework as a catalyst for the synthesis of cyclic carbonates by CO_2 cycloaddition, *J. Ind. Eng. Chem.*, 2020, **89**, 104-110.
23. J. W. Lan, Y. Qu, Z. J. Wang, P. Xu and J. M. Sun, A facile fabrication of a multi-functional and hierarchical Zn-based MOF as an efficient catalyst for CO_2 fixation at room-temperature, *Inorg. Chem. Front.*, 2021, **8**, 3085–3095.